

To appear in ApJ

The most massive core collapse supernova progenitors

R. Waldman

Racah Institute of Physics, The Hebrew University, Jerusalem 91904, Israel

waldman@cc.huji.ac.il

ABSTRACT

The discovery of the extremely luminous supernova SN 2006gy, possibly interpreted as a pair instability supernova, renewed the interest in very massive stars. We explore the evolution of these objects, which end their life as pair instability supernovae or as core collapse supernovae with relatively massive iron cores, up to about $3 M_{\odot}$.

Subject headings: stars: evolution, (stars:) supernovae: general

1. Introduction

The interest in the evolution of very massive stars (VMS), with masses $\gtrsim 100 M_{\odot}$, has recently been revived by the discovery of SN 2006gy - the most luminous supernova ever recorded (Ofek et al. 2007; Smith et al. 2007). This object, having a luminosity of ~ 10 times that of a typical core-collapse SN (CCSN), is probably the first evidence of a pair instability SN (PISN) Woosley et al. (2007). PISN are massive stellar objects, whose evolutionary path brings their center into a region in thermodynamical phase space ($\rho \lesssim 10^6$, $T \gtrsim 10^9$), where thermal energy is converted into the production of electron-positron pairs, thus resulting in loss of pressure and hydrodynamic instability. This type of supernova was first suggested 40 years ago by Rakavy & Shaviv (1967); Barkat et al. (1967), and since then several works were carried out (e.g. Fraley 1968; Ober et al. 1983; El Eid et al. 1983; Bond et al. 1984; Heger & Woosley 2002; Hirschi et al. 2004; Eldridge & Tout 2004; Nomoto et al. 2005), however the overall interest in this topic has been relatively small, mainly due to lack of observational data.

It was originally believed that stars massive enough to produce PISN could only be found among population III stars with close to zero metallicity ($Z \lesssim 10^{-4}$), and hence

only at very high redshift ($z \gtrsim 15$). More recently Scannapieco et al. (2005) discussed the detectability of PISN at redshift of $z \leq 6$, arguing that metal enrichment is a local process, therefore metal-free star-forming pockets may be found at such low redshifts. Langer et al. (2007) introduced the effect of rotation into studying this question concluding that PISN could be produced by slow rotators of metallicity $Z \lesssim Z_{\odot}/3$ at a rate of one in every 1000 SN in the local universe. Furthermore, Smith et al. (2007) point out, that mass loss rates in the local universe might be much lower than previously thought, so that massive stars might be left with enough mass to become PISN. This conclusion is also supported by Yungelson et al. (2008) who extensively discuss the mass loss rates and fates of VMS. It is interesting to note, that SN 2006gy took place in the nearby Universe. Following the discovery of SN 2006gy, Umeda & Nomoto (2008) addressed the question of how much ^{56}Ni can be produced in massive CCSN, while Heger & Woosley (2008) computed the detailed nucleosynthesis in these SNe.

The interest in VMS is further motivated by the discovery of Ultraluminous X-ray Sources (ULX), which can be interpreted as mass-accreting intermediate mass black holes (IMBH) with mass $\sim (10^2 - 10^5) M_{\odot}$. One of the possible scenarios for IMBH formation is by VMS formed by stellar mergers in compact globular clusters (see e.g. Yungelson et al. 2008, and references therein). In this context, Nakazato et al. (2006, 2007) studied the collapse of massive iron cores with $M \gtrsim 3 M_{\odot}$. In their first paper they treat the fate of stars of mass $\geq 300 M_{\odot}$ which reach the photodisintegration temperature ($\approx 6 \times 10^9 K$) after undergoing pair instability. The entropy per baryon of these models at photodisintegration is $s > 16 k_B$ compared with the classical core-collapse SN with $s \sim 1 k_B$. In the second paper they aim to bridge this entropy gap, corresponding to core masses of $(3 - 30) M_{\odot}$ but claim that there is a lack of systematic progenitor models for this range, hence they use synthetic initial models for their calculations.

In this work we focus mostly on the mass range $M \lesssim 80 M_{\odot}$ (He core mass $M_{\text{He}} \lesssim 36 M_{\odot}$) immediately below the range which enters the pair instability region, and present a systematic picture of the resulting CCSN progenitors.

2. Method

Since the mass loss rates of stars in this range are highly uncertain, (see e.g. discussion by Yungelson et al. 2008), we avoid dealing with this question by following the example of Heger & Woosley (2002), and modeling the evolution of helium cores. Our helium core initial models are homogeneous polytropes composed entirely of helium and metals, with metallicity $Z \approx 0.015$, in the mass range $(8 - 160) M_{\odot}$. The models were then evolved to

the helium zero age main sequence. In the following we will refer to these models as “He N ” where N is the mass of the model. For comparison we evolved also a few models of regular hydrogen stars, beginning from the zero-age main sequence (ZAMS). We will refer to these models as “MN” where N is the mass of the model. All our models have no mass-loss. We argue that as long as the mass loss rate is not so high that it will cut into the He-core, the evolution after the main-sequence phase will be virtually independent of the fate of the hydrogen-rich envelope. We followed the evolution of each model until the star is either completely disrupted (for the PISN case) or Fe begins to photo-disintegrate (for the CCSN case).

We followed the evolution using the Lagrangian one dimensional Tycho evolutionary code version 6.92 (with some modifications), publicly available on the web (the code is described in Young & Arnett 2005). Convection is treated using the well known mixing length theory (MLT) with the Ledoux criterion. In the MLT formulation of Tycho, the value of the mixing length parameter fit to the Sun is $\alpha_{MLT} \approx 2.1$ (Young & Arnett 2005), so we used a value of $\alpha_{MLT} = 2$ in our calculations. The nuclear reaction rates used by TYCHO are taken from the NON-SMOKER database as described in Rauscher & Thielemann (2000).

The evolution is generally followed using the code’s hydrostatic mode. The pulsational pair instability models are treated as follows. When hydrodynamic instability is encountered, the code is switched to the hydrodynamic mode, and mass ejection is accounted for by removing outer zones having supersonic velocity in excess of the escape velocity. After mass ejection has died out, and the stellar core is already in contraction, the code is switched back to the hydrostatic mode to follow the interpulse period.

3. Results

The He-core models we computed can be divided into four categories, according to their final fate, as can be seen in the central density and temperature plot (Fig. 1):

1. CCSN - Models that reach core collapse (i.e. Fe photo-disintegration) conditions without entering the region of pair instability. This is the fate of He-cores with mass $M \leq 36 M_{\odot}$, as can be seen for the models He8 and He36 in Fig. 1.
2. Pulsational PISN (PPI)- Models that reach pair instability, collapse and bounce due to the energy released by nuclear reactions, but the energy released is insufficient to disrupt the entire star, thus a fraction of the star’s mass is emitted, and the star collapses back. This may happen several times, until the star has no more material to

burn and reverse the collapse, and core collapse conditions are reached. This occurs for models with He-core mass in the range $36 < M \leq 54 M_{\odot}$, e.g. model He48 in Fig. 1.

3. PISN - Models that reach pair instability, collapse, and the energy released by nuclear reactions is high enough to disrupt the entire star. This occurs for models with He-core mass in the range $54 < M \lesssim 130 M_{\odot}$, e.g. model He80 in Fig. 1.
4. Pair instability core collapse (PICC) - Models that reach pair instability, but the energy released is too low to reverse the collapse, and the star continues collapsing into the photodisintegration regime. This occurs for models with He-core mass in the range $M \gtrsim 130 M_{\odot}$, e.g. model He160 in Fig. 1.

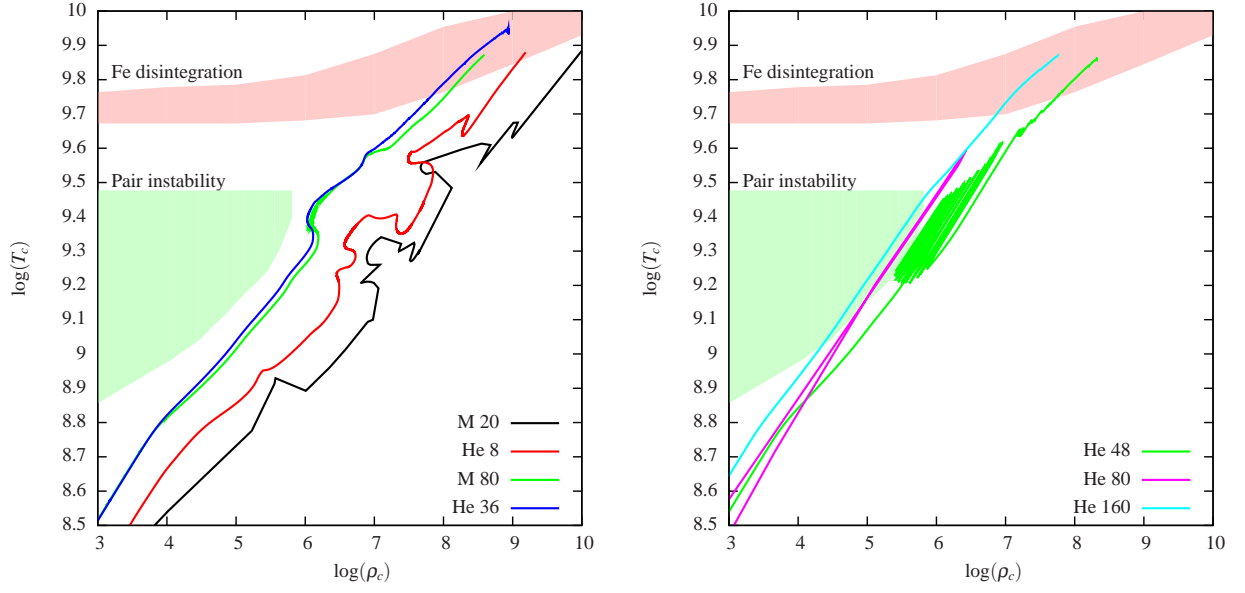


Fig. 1.— Evolution of the central density and temperature. Each line is labeled “M” for stellar models and “He” for He-core models, followed by the mass of the model. The figure is divided into two panels for clarity - the left panel shows models that reach CC without reaching pair instability, the right panel shows models reaching pair instability, subsequently experiencing pulsations (He48), complete disruption (He80), or direct collapse (He160).

The properties of our models at pre-SN are summarized in table 1.

Table 1. Properties of the pre-SN models.

Model	M	M_{He}	M_{CO}	M_{Si}	M_{Fe}	X_{C12}	X_{Ne20}	ρ_c	T_c	S_c	Y_e	E_{bin}	SN type
M20	20	6.1	2.71	2.05	1.44	0.200	0.003	5.9E+09	7.0	0.70	0.424	0.8	CC
M80	80	37.5	28.20	10.20	2.80	0.050	0.066	2.8E+08	7.0	1.64	0.454	3.9	CC
M100	100	50.4	38.90	20.10	2.53	0.037	0.081	2.5E+08	7.0	1.72	0.454	4.0	CC
He8		8.0	5.7	2.25	1.62	0.158	0.008	1.1E+09	7.0	1.05	0.440	1.2	CC
He12		12.0	8.8	3.84	1.98	0.124	0.014	7.1E+08	7.0	1.18	0.443	1.7	CC
He16		16.0	11.9	4.01	1.88	0.100	0.021	5.9E+08	7.0	1.25	0.444	2.2	CC
He20		20.0	15.4	5.04	2.01	0.079	0.031	4.9E+08	7.0	1.33	0.447	2.7	CC
He24		24.0	18.6	6.34	2.15	0.072	0.036	3.8E+08	7.0	1.45	0.449	3.1	CC
He28		28.0	22.0	7.99	2.25	0.063	0.044	3.0E+08	7.0	1.60	0.452	3.5	CC
He32		32.0	25.5	9.79	2.18	0.056	0.051	2.3E+08	7.0	1.77	0.456	3.5	CC
He34		34.0	27.3	11.20	2.42	0.053	0.054	2.1E+08	7.0	1.84	0.456	3.6	CC
He36		36.0	29.1	12.10	2.88	0.050	0.057	2.0E+08	7.0	1.91	0.457	3.7	CC
He38		38.0	30.8	13.00	2.67	0.048	0.060	1.8E+08	7.0	1.97	0.457	3.6	PPI
He44		44.0	35.7	10.80	2.65	0.042	0.069	2.1E+08	7.0	1.86	0.457	3.4	PPI
He48		48.0	39.1	17.00	2.96	0.039	0.074	1.7E+08	7.0	2.00	0.458	3.1	PPI
He50		50.0	40.9	14.50	3.05			1.8E+08	7.0	1.97	0.459	4.1	PPI
He52		52.0	42.5	10.50	2.76			1.1E+09	7.0	1.03	0.439	2.5	PPI
He54		54.0	44.3	18.80	2.81			1.2E+09	7.0	1.04	0.439	2.9	PPI
He56		56.0	46.00			0.034	0.084	5.7E+05	2.0			5.3	PISN
He64		64.0	53.00					3.7E+05	1.9			5.8	PISN
He72		72.0	60.00					2.7E+05	1.8			6.4	PISN
He80		80.0	67.00					2.2E+05	1.7			7.0	PISN
He96		96.0	82.00					1.5E+05	1.6			8.1	PISN
He128		128.0	110.00					7.6E+04	1.4			10.0	PISN
He160		160.0	144.00					5.3E+04	1.4			12.0	PICC

Note. — The columns represent for each model the total mass (M), He-core mass (M_{He}), CO-core mass (M_{CO}), Si-core mass (M_{Si}), Fe-core mass (M_{Fe}), ^{12}C and ^{20}Ne mass fraction at the end of core He burning (X_{C12} and X_{Ne20}), central density (ρ_c), temperature (T_c), entropy per baryon (S_c), electron mole fraction (Y_e), and binding energy (E_{bin}). Masses are given in M_\odot , density in $g\,cm^{-3}$, temperature in $10^9\,K$, and energy in $10^{51}\,erg$. For the models reaching core collapse the data are given

when central temperature reaches 7×10^9 , while for the models that disrupt after reaching pair instability the data are given at onset of instability.

Fig. 2 shows the density structure of the pre-SN, at the moment when the central temperature reaches $7 \times 10^9 K$. The two extreme models He8 and He36 are shown, as well as M80 which has a He-core mass similar to the He36 model, and M20 - a typical CCSN progenitor. The composition of the same models is shown in Fig. 3.

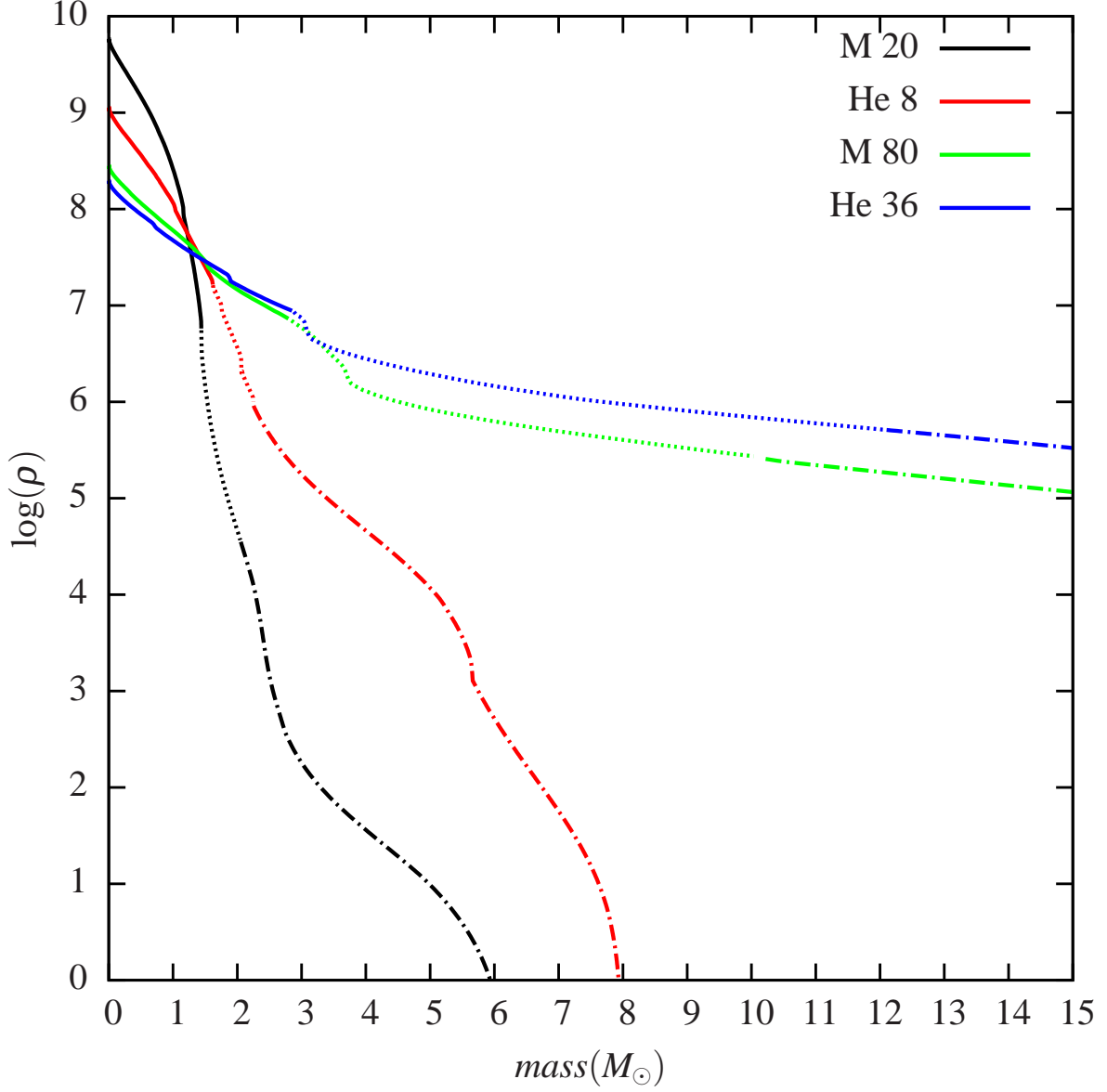


Fig. 2.— Pre-SN density structure. Each line is labeled “M” for stellar models and “He” for He-core models, followed by the mass of the model. (In the color version the solid part of each line designates the Fe-group core, the dotted part - the Si-group core, and the dash-dotted - the rest of the model.)

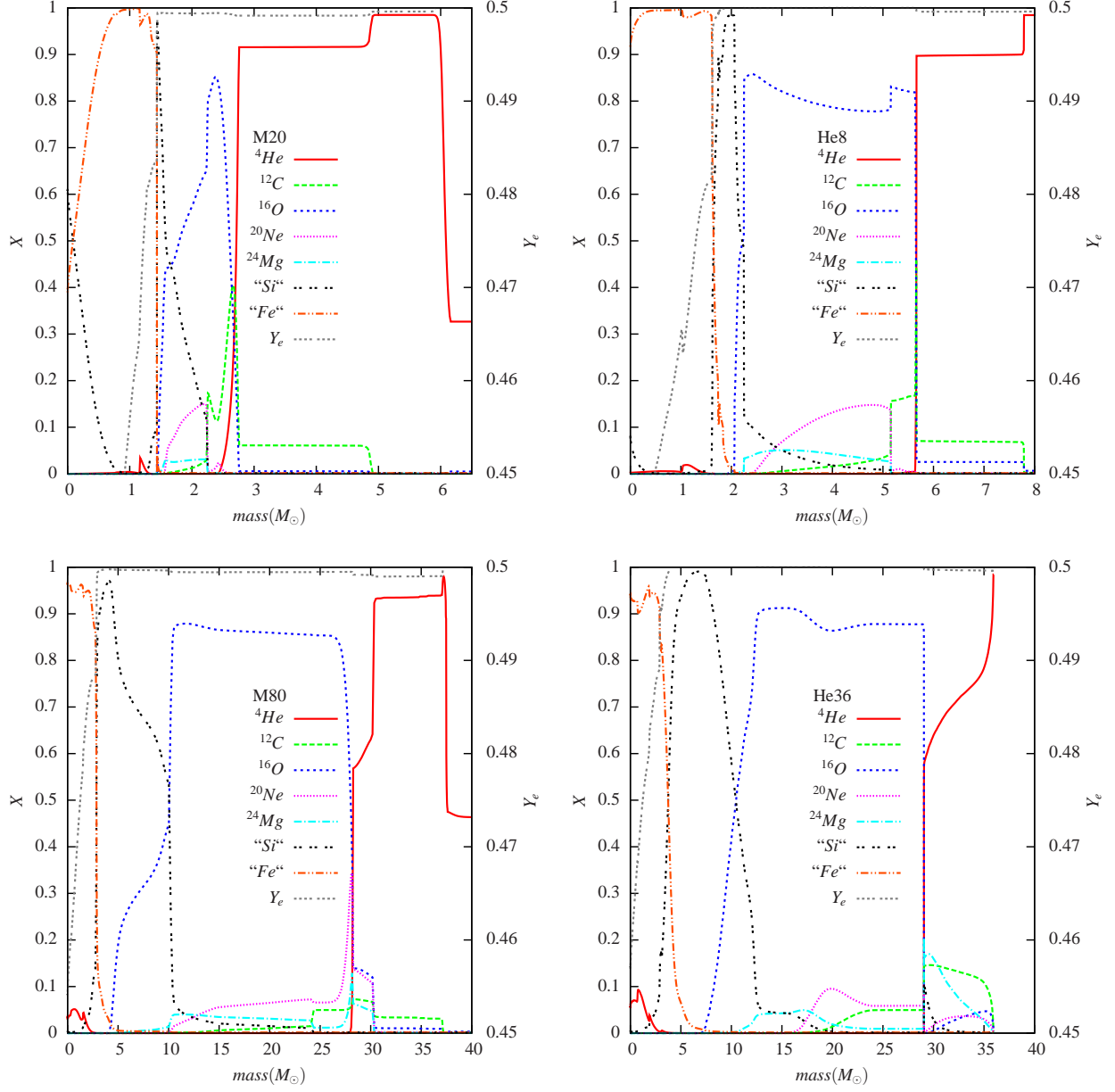


Fig. 3.— Pre-SN composition of models M20, He8, M80 and He36. “Si” and “Fe” stand for the total of Si- and Fe-group elements respectively.

The size of the Fe-, Si-, and CO-cores of our pre-SN models is shown in Fig. 4 plotted against the size of the He-core. A scaled-up view of the size of the Fe-core (defined as the mass coordinate where the electron mole fraction $Y_e < 0.49$) together with the central entropy per baryon for the same models is shown in Fig. 5. Note that the size of the Fe-core is slightly non-monotonic. The central entropy, is monotonic with mass, but slightly differs between He-core and stellar models.

From the above results it is notable that the He-core models behave similarly to the stellar models (compare e.g. models He36 and M80 which has a He-core mass of $\approx 36 M_\odot$), however some differences still exist (e.g. the central entropy in Fig. 5).

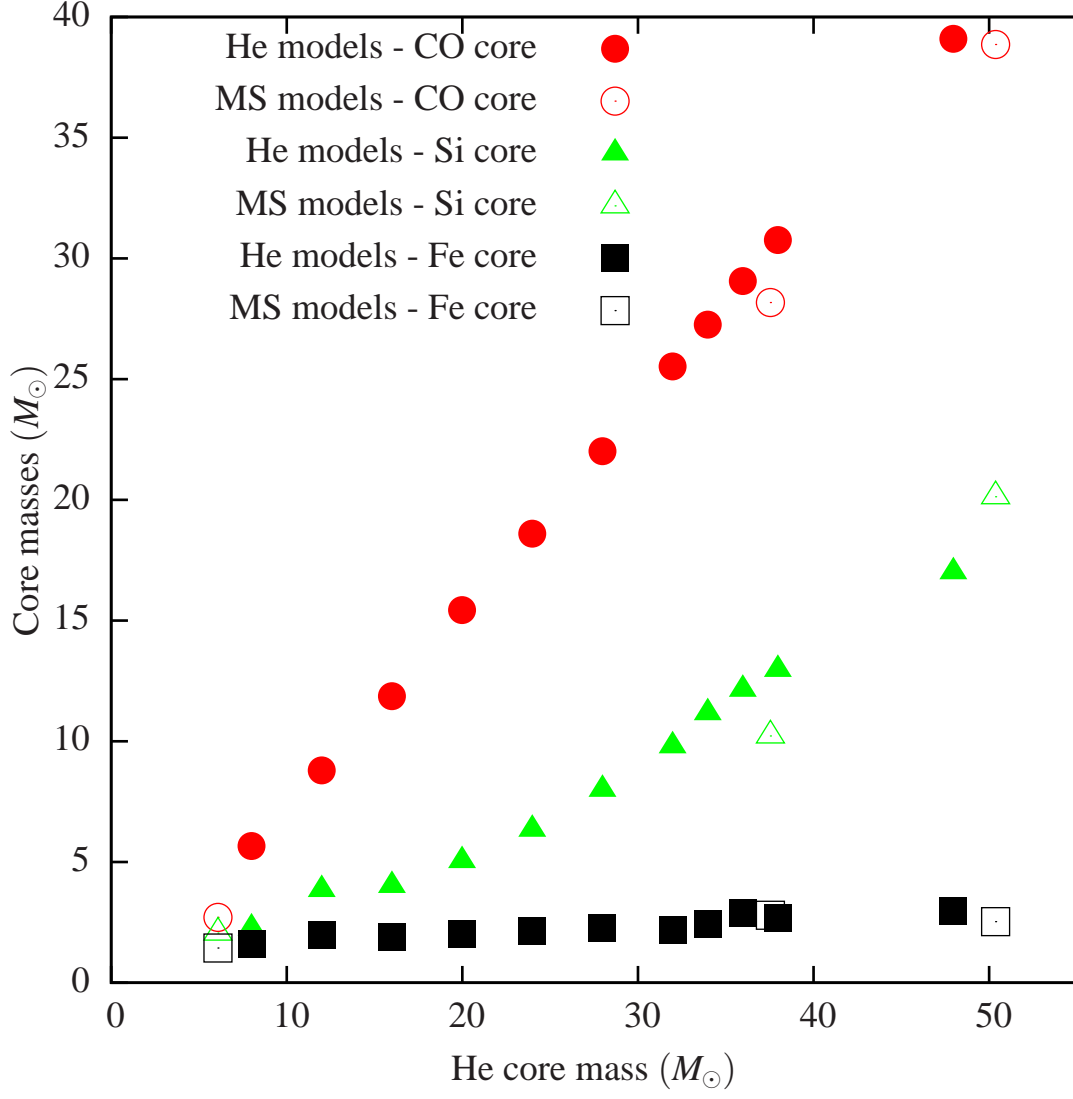


Fig. 4.— Mass of the Fe-core (squares), Si-core (triangles), and CO-core(circles) for the computed models. Filled shapes designate He-core models, open shapes - stellar models.

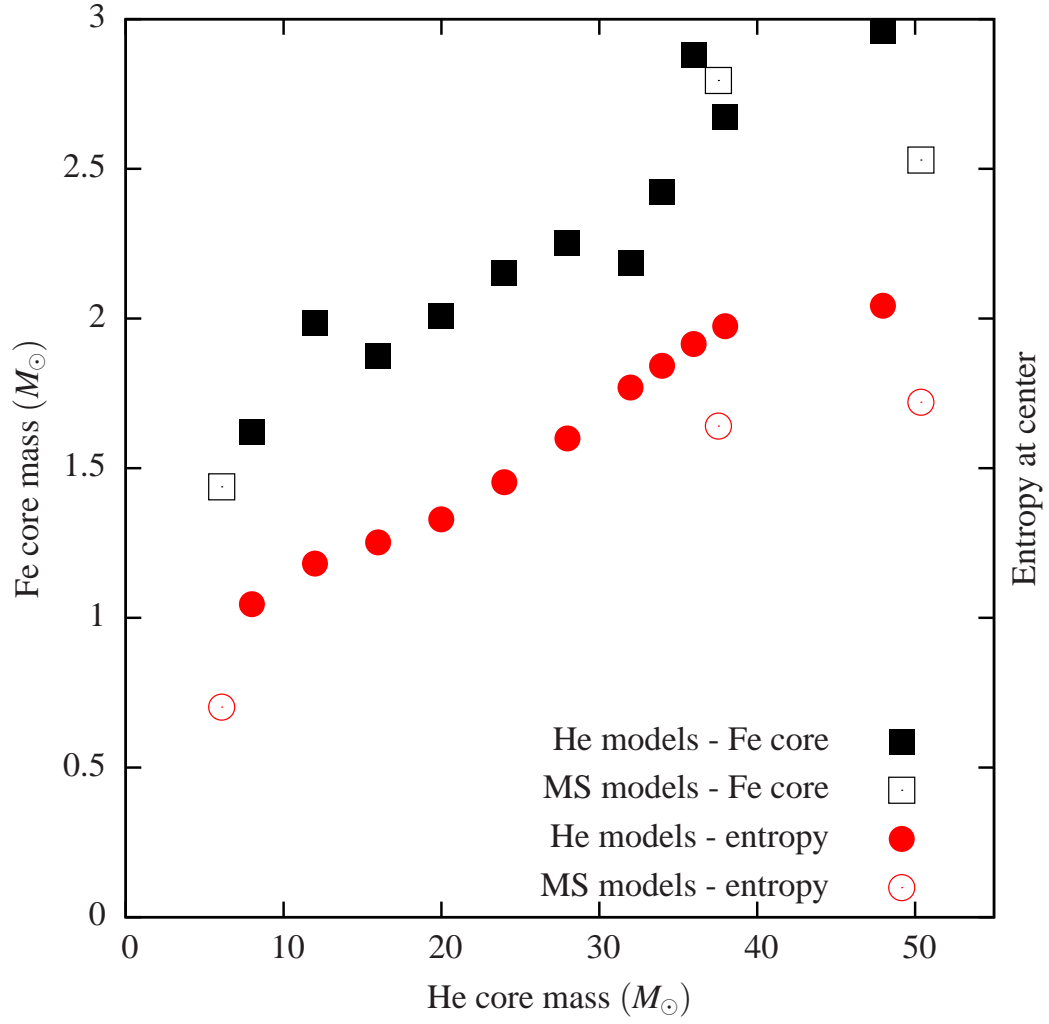


Fig. 5.— Mass of the Fe-core (squares) and central entropy per baryon (circles) for the computed models. Filled shapes designate He-core models, open shapes - stellar models.

4. Conclusions

Our results are in general agreement with previously published results (e.g. Heger & Woosley 2002; Woosley et al. 2007; Umeda & Nomoto 2008). We focused on the heaviest models which do not encounter pair instability (CCSN) in the range (He8 - He36). The outstanding novel features of these models are:

1. Relatively large Fe-cores, up to about $3 M_{\odot}$, and a large amount (up to about $10 M_{\odot}$) of Si-group elements.
2. Comparatively low central density and high central entropy.
3. A comparatively shallow density profile.

These differences might have a considerable impact on the behavior of these models during core collapse and on the outcome of the explosion, a question which we hope to address in the future.

Similar features are encountered for the lower mass part of the pulsational pair instability models (He38 - He50). However, due to the numerical complexity of following the pulsations and the potential sensitivity of the results to the numerical treatment of convection, mass loss etc., further work is needed to ascertain the validity of the results for the pulsational models.

I would like to thank Zalman Barkat for many hours of fruitful discussion. I would like to acknowledge David Arnett for providing his TYCHO code for public use.

REFERENCES

- Barkat, Z., Rakavy, G., & Sack, N. 1967, Phys. Rev. Lett., 18, 379
- Bond, J. R., Arnett, W. D., & Carr, B. J. 1984, ApJ, 280, 825
- El Eid, M. F., Fricke, K. J., & Ober, W. W. 1983, A&A, 119, 54
- Eldridge, J. J., & Tout, C. A. 2004, MNRAS, 353, 87
- Fraley, G. S. 1968, Ap&SS, 2, 96
- Heger, A., & Woosley, S. E. 2002, ApJ, 567, 532

- . 2008, ArXiv e-prints, 803
- Hirschi, R., Meynet, G., & Maeder, A. 2004, *A&A*, 425, 649
- Langer, N., Norman, C. A., de Koter, A., Vink, J. S., Cantiello, M., & Yoon, S.-C. 2007, *A&A*, 475, L19
- Nakazato, K., Sumiyoshi, K., & Yamada, S. 2006, *ApJ*, 645, 519
- . 2007, *ApJ*, 666, 1140
- Nomoto, K., Tominaga, N., Umeda, H., Maeda, K., Ohkubo, T., Deng, J., & Mazzali, P. A. 2005, in *Astronomical Society of the Pacific Conference Series*, Vol. 332, *The Fate of the Most Massive Stars*, ed. R. Humphreys & K. Stanek, 374–+
- Ober, W. W., El Eid, M. F., & Fricke, K. J. 1983, *A&A*, 119, 61
- Ofek, E. O., Cameron, P. B., Kasliwal, M. M., Gal-Yam, A., Rau, A., Kulkarni, S. R., Frail, D. A., Chandra, P., Cenko, S. B., Soderberg, A. M., & Immler, S. 2007, *ApJ*, 659, L13
- Rakavy, G., & Shaviv, G. 1967, *ApJ*, 148, 803
- Rauscher, T., & Thielemann, F.-K. 2000, *Atomic Data and Nuclear Data Tables*, 75, 1
- Scannapieco, E., Madau, P., Woosley, S., Heger, A., & Ferrara, A. 2005, *ApJ*, 633, 1031
- Smith, N., Li, W., Foley, R. J., Wheeler, J. C., Pooley, D., Chornock, R., Filippenko, A. V., Silverman, J. M., Quimby, R., Bloom, J. S., & Hansen, C. 2007, *ApJ*, 666, 1116
- Umeda, H., & Nomoto, K. 2008, *ApJ*, 673, 1014
- Woosley, S. E., Blinnikov, S., & Heger, A. 2007, *Nature*, 450, 390
- Young, P. A., & Arnett, D. 2005, *ApJ*, 618, 908
- Yungelson, L. R., van den Heuvel, E. P. J., Vink, J. S., Portegies Zwart, S. F., & de Koter, A. 2008, *A&A*, 477, 223